Figure S1

A

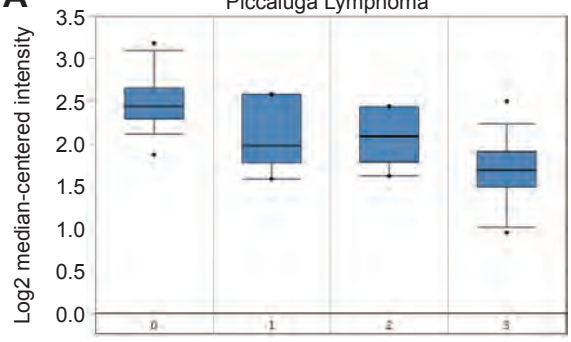

0. No value (20)
1. Anaplastic large cell lymphoma (6)
2. Angioimmunoblastic T-cell lymphoma (6)
3. Unspecified Peripheral T-cell lymphoma (28)

B

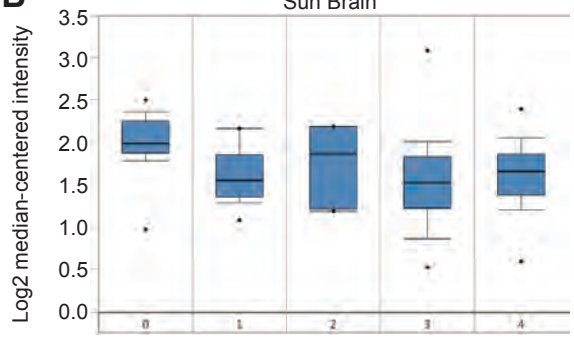

0. No value (23)
1. Anaplastic astrocytoma (19)
2. Diffuse astrocytoma (7)
3. Glioblastoma (81)
4. Oliogodendroglioma (50)

C

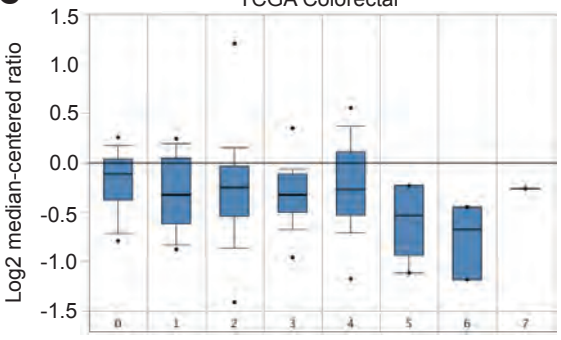

0. No value (22)
1. Cecum adenocarcinoma (22)
2. Colon adenocarcinoma (101)
3. Colon mucinous adenocarcinoma (22)
4. Rectal adenocarcinoma (60)
5. Rectal mucinous adenocarcinoma (6)
6. Rectosigmoid adenocarcinoma (3)
7. Rectosigmoid mucinous adenocarcinoma (1)

D

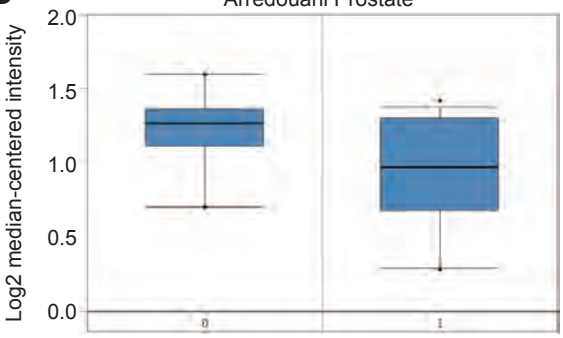

0. No value (8)
1. Prostate carcinoma (13)

E

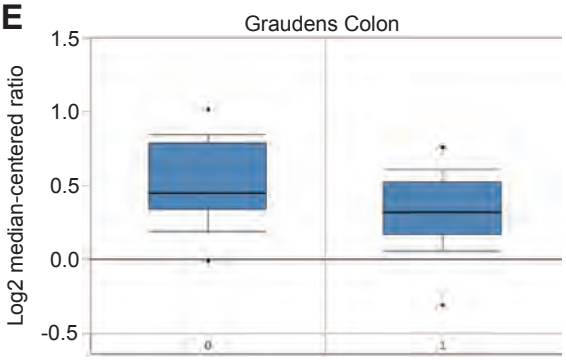

0. No value (12)
1. Colorectal carcinoma (46)

F

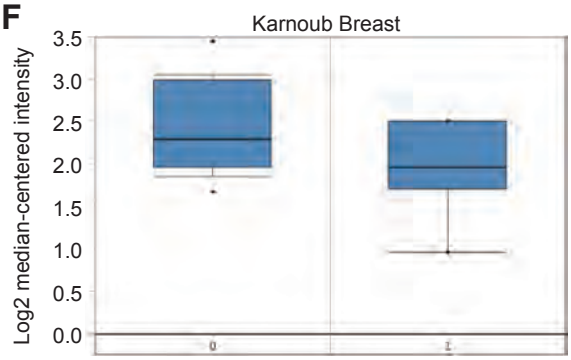

0. No value (15)
1. Invasive ductal breast carcinoma (7)

G

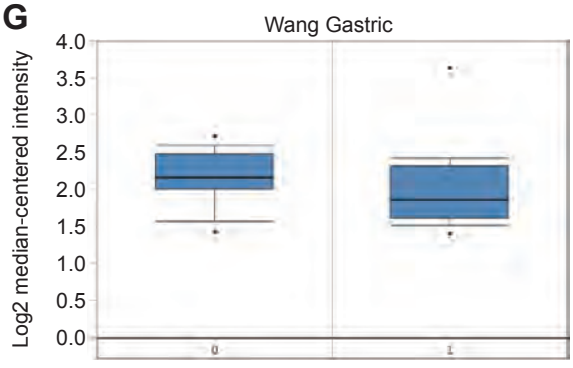

0. No value (15)
1.Gastric cancer (12)

A

```
HeLa                GCAGTCTCATTATGGGACACCGTACCCCAGCCACCTGGGCCCAGTGGGCATGGGCAACAG
CRTC2 KO1-Allele1 GCAGTCTCATTATGGGACACCGTACT-----CACCTGGGCCCAGTGGGCATGGGCAACAG
CRTC2 KO1-Allele2 GCAGTCTCATTATGGGACACCGTACTC---------TGGGCCCAGTGGGCATGGGCAACAG
CRTC2 KO2-Allele1 GCAGTCTCATTATGGGACACCGTAC----------TGGGCCCAGTGGGCATGGGCAACAG
CRTC2 KO2-Allele2 GCAGTCTCATTATGGGACACCGTACCCCA----CCTGGGCCCAGTGGGCATGGGCAACAG
```

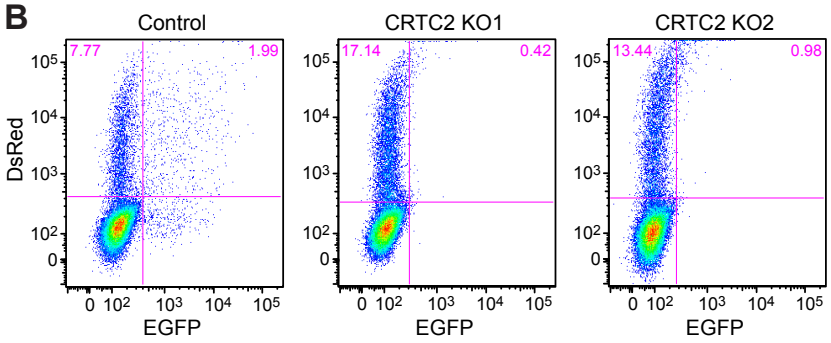

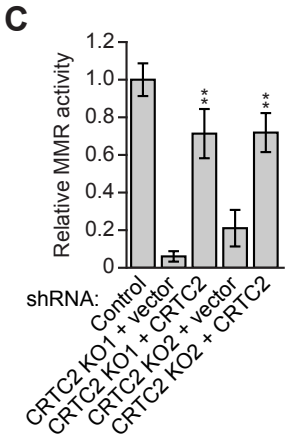

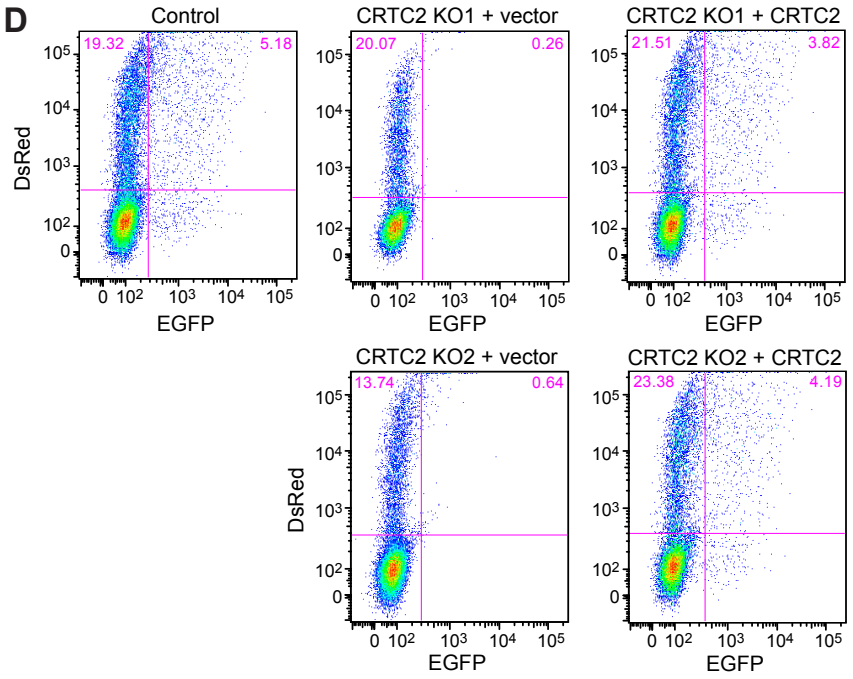

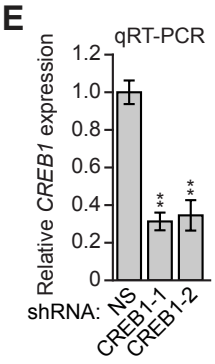

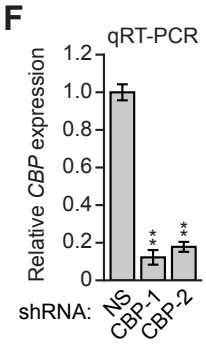

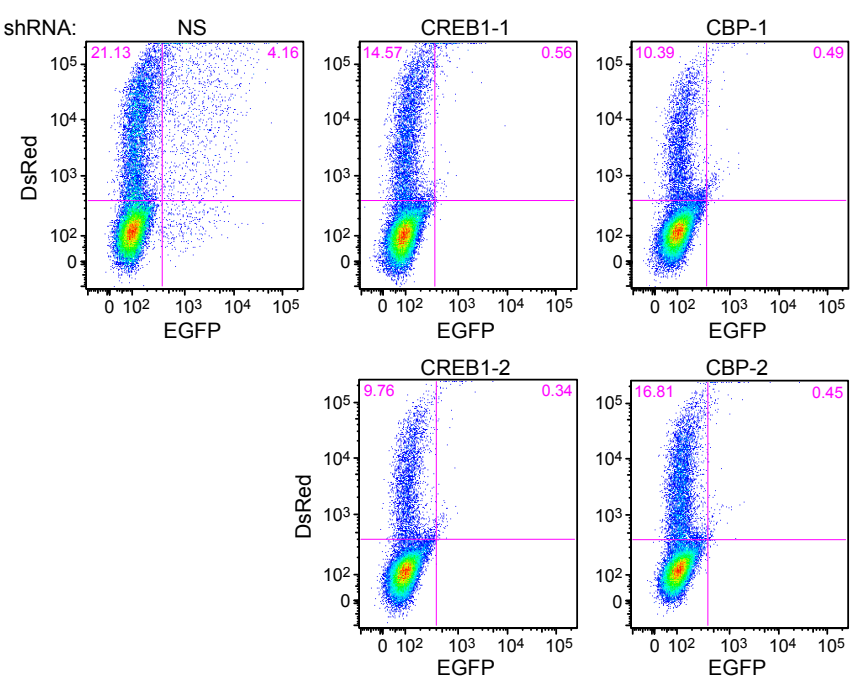

Figure S3

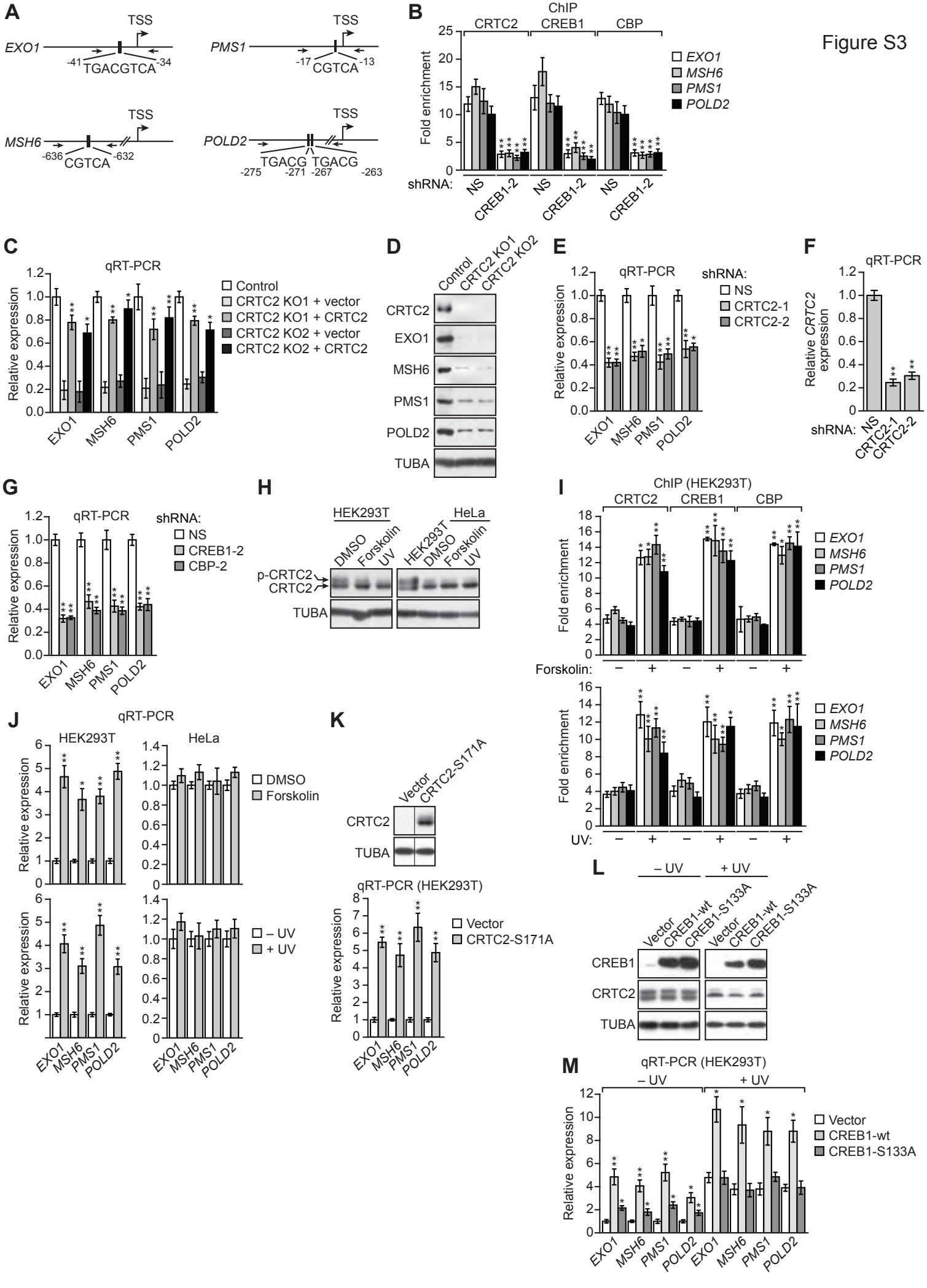
A
TSS
EXO1
-41 TGACGTCA -34
PMS1
-17 CGTCA -13
MSH6
-636 CGTCA -632
POLD2
-275 -271 -267 TGACG TGACG -263
B
ChIP
CRTC2
CREB1
CBP
Fold enrichment
shRNA: NS CREB1-2
EXO1
MSH6
PMS1
POLD2
C
qRT-PCR
Relative expression
Control
CRTC2 KO1 + vector
CRTC2 KO1 + CRTC2
CRTC2 KO2 + vector
CRTC2 KO2 + CRTC2
D
Control
CRTC2 KO1
CRTC2 KO2
CRTC2
EXO1
MSH6
PMS1
POLD2
TUBA
E
qRT-PCR
shRNA:
NS
CRTC2-1
CRTC2-2
F
qRT-PCR
Relative CRTC2 expression
G
qRT-PCR
shRNA:
NS
CREB1-2
CBP-2
H
HEK293T
HeLa
DMSO
Forskolin
UV
p-CRTC2
CRTC2
TUBA
I
ChIP (HEK293T)
Forskolin:
UV:
J
qRT-PCR
HEK293T
HeLa
DMSO
Forskolin
– UV
+ UV
K
Vector
CRTC2-S171A
CRTC2
TUBA
qRT-PCR (HEK293T)
L
– UV
+ UV
Vector
CREB1-wt
CREB1-S133A
CREB1
CRTC2
TUBA
M
qRT-PCR (HEK293T)
– UV
+ UV

Figure S4

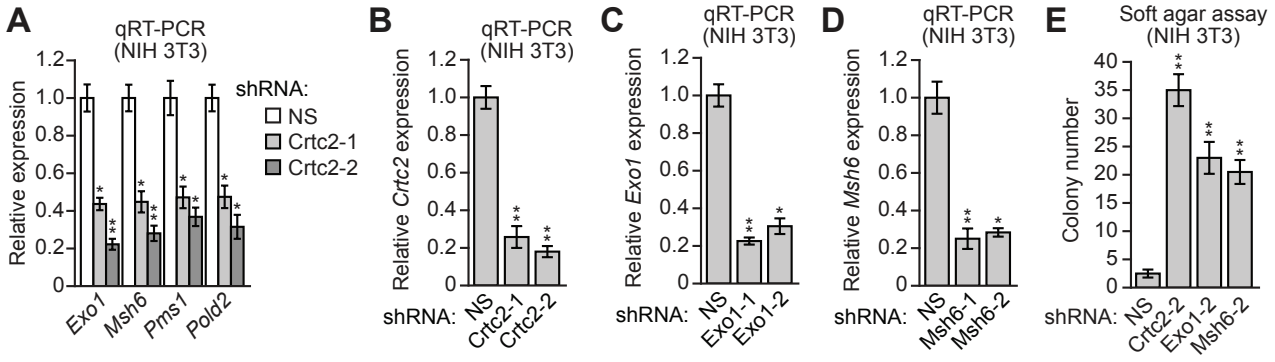
A
qRT-PCR
(NIH 3T3)
Relative expression
shRNA:
NS
Crtc2-1
Crtc2-2
Exo1
Msh6
Pms1
Pold2
B
qRT-PCR
(NIH 3T3)
Relative Crtc2 expression
shRNA:
NS
Crtc2-1
Crtc2-2
C
qRT-PCR
(NIH 3T3)
Relative Exo1 expression
shRNA:
NS
Exo1-1
Exo1-2
D
qRT-PCR
(NIH 3T3)
Relative Msh6 expression
shRNA:
NS
Msh6-1
Msh6-2
E
Soft agar assay
(NIH 3T3)
Colony number
shRNA:
NS
Crtc2-2
Exo1-2
Msh6-2

SUPPLEMENTAL FIGURE LEGENDS

Figure S1. *CRTC2* is Down-regulated in Multiple Cancers (Related to Figure 1)
(A-E) Representative boxplots from Oncomine data analysis showing *CRTC2* is significantly down-regulated (P<1E-4, fold change>2) in cancer versus normal tissue for lymphoma (Piccaluga et al., 2007), brain (Sun et al., 2006), colorectal (Graudens et al., 2006), prostate (Arredouani et al., 2009), breast (Karnoub et al., 2007) and gastric (Wang et al., 2012) cancers. The Oncomine data analysis revealed that the most significant downregulation of *CRTC2* occurred in the Piccaluga lymphoma samples.

Figure S2. Additional Experiments Related to Figure 1
(A) Sequence analysis of both alleles in each of the two CRTC2 KO HeLa cell lines. The results confirmed that both alleles in each cell line were disrupted, and that the deletions resulted in a frameshift, leading to a premature stop codon.
(B) Representative FACS plots showing the percentage of EGFP-positive, DsRed-positive and EGFP-negative, DsRed-positive cells sorted from control HeLa and CRTC2 KO1 and KO2 HeLa cells co-transfected with an EGFP heteroduplexed mismatch plasmid and DsRed-N1.
(C) MMR activity assay in control HeLa cells or CRTC2 KO HeLa cells expressing CRTC2 or empty vector.
(D) Representative FACS plots showing the percentage of EGFP-positive, DsRed-positive, and EGFP-negative, DsRed-positive cells sorted from CRTC2 KO HeLa cells expressing CRTC2 or empty vector and co-transfected with an EGFP heteroduplexed mismatch plasmid and DsRed-N1.
(E,F) qRT-PCR analysis monitoring knockdown efficiency of *CREB1* (E) and *CBP* (F) in HeLa cells expressing a non-silencing (NS) shRNA or one of two CREB1 or CBP shRNAs. For all graphs, error bars indicate standard deviation. $^{**}P$<0.01.
(G) Representative FACS plots showing the percentage of EGFP-positive, DsRed-positive, and EGFP-negative, DsRed-positive cells sorted from HeLa cells expressing a NS, CREB1 or CBP shRNA and co-transfected with an EGFP heteroduplexed mismatch plasmid and DsRed-N1.

Figure S3. Schematic Diagrams and Additional Experiments Related to Figure 2
(A) Schematic diagrams showing the position and sequence of the CRE site, either an octameric palindrome (5'-TGACGTCA-3') or a less active half-site motif (5'-TGACG-3' or 5'-CGTCA-3') (Mayr and Montminy, 2001), in the promoters of *EXO1*, *MSH6*, *PMS1* and *POLD2*.
(B) ChIP analysis monitoring occupancy of CRTC2, CREB1 and CBP on the promoters of *EXO1*, *MSH6*, *PMS1* and *POLD2* in HeLa cells expressing a NS shRNA or a CREB1 shRNA unrelated to that shown in Fig. 2B.
(C) qRT-PCR analysis monitoring expression of *EXO1*, *MSH6*, *PMS1* and *POLD2* in control HeLa cells or CRTC2 KO HeLa cells expressing CRTC2 or empty vector.
(D) Immunoblot analysis monitoring levels of CRTC2, EXO1, MSH6, PMS1 and POLD2 in control HeLa cells and CRTC2 KO HeLa cells. α-tubulin (TUBA) was monitored as a loading control.
(E) qRT-PCR analysis monitoring expression of *EXO1*, *MSH6*, *PMS1* and *POLD2* in HeLa cells expressing an NS shRNA or one of two unrelated CRTC2 shRNAs.
(F) qRT-PCR analysis monitoring knockdown efficiency of *CRTC2* in HeLa cells expressing an NS or CRTC2 shRNA.

(G) qRT-PCR analysis monitoring expression of *EXO1*, *MSH6*, *PMS1* and *POLD2* in HeLa cells expressing an NS shRNA or CREB1 or CBP shRNA unrelated to that used in Fig. 2D.
(H) Immunoblot analysis monitoring CRTC2 phosphorylation in HeK293T or HeLa cells treated with DMSO, forskolin or UV. CRTC2 phosphorylation was monitored by mobility shift. These blots used 5% gels and long running times to optimize the resolution of the two bands; the top band represents phosphorylated CRTC2 (p-CRTC2) and the bottom band represents the unphosphorylated form. α-tubulin (TUBA) was monitored as a loading control.
(I) ChIP analysis monitoring occupancy of CRTC2, CREB1 and CBP on the promoters of *EXO1*, *MSH6*, *PMS1* and *POLD2* in HEK293T cells treated in the presence or absence of forskolin.
(J) qRT-PCR analysis monitoring expression of *EXO1*, *MSH6*, *PMS1* and *POLD2* in HEK293T or HeLa cells treated in the presence or absence of UV.
(K) (Top) Immunoblot analysis confirming ectopic expression of the CRTC2-S171A mutant. Non-adjacent lanes from the same gel were spliced together as indicated by the dividing line. (Bottom) qRT-PCR analysis monitoring expression of *EXO1*, *MSH6*, *PMS1* and *POLD2* in HEK293T cells expressing empty vector (pcDNA3.1) or CRTC2-S171A.
(L) Immunoblot analysis monitoring CREB1 levels in HEK293T cells expressing empty vector (pcDNA3.1), wild-type CREB1 (CREB1-wt) or CREB1-S133A and treated with or without UV 30 J/m^2 24 hours post transfection. CRTC2 phosphorylation was also monitored; as expected, dephosphorylation of CRTC2 following UV irradiation was equivalent in the presence of wild type CREB1 or CREB1-S133A.
(M) qRT-PCR analysis monitoring expression of *EXO1*, *MSH6*, *PMS1* and *POLD2* in HEK293T cells expressing empty vector, CREB1-wt or CREB1-S133A and treated in the presence or absence of UV. For all graphs, error bars indicate SD. **P*<0.05, ***P*<0.01.

Figure S4. Additional Experiments Related to Figure 3
(A) qRT-PCR analysis monitoring expression of *Exo1*, *Msh6*, *Pms1* and *Pold2* in NIH 3T3 cells expressing an NS shRNA or one of two unrelated Crtc2 shRNAs.
(B-D) qRT-PCR analysis monitoring knockdown efficiency of *Crtc2* (B), *Exo1* (C) or *Msh6* (D) in NIH 3T3 cells expressing an NS shRNA or one of two unrelated *Crtc2*, *Exo1* or *Msh6* shRNAs.
(E) Soft agar assay monitoring colony forming ability of NIH 3T3 cells expressing a NS, *Crtc2*, *Exo1* or *Msh6* shRNA unrelated to that used in Fig. 3A. For all graphs, error bars indicate SD. **P*<0.05, ***P*<0.01.

Table S1. List of mutations in *CRTC2* (transcript ENST00000368633) Found in the COSMIC Database (Related to Figure 1)

Please see the accompanying Excel file.

Table S2. List of Lymphoma Samples Used in this Study (Related to Figure 3)
The diagnosis, source tissue and, for formalin-fixed paraffin embedded (FFPE) samples, whether or not CRTC2 could be detected by immunohistochemistry (IHC) are given. ALCL, anaplastic large cell lymphoma, ATCL, angioimmunoblastic T-cell lymphoma, PTCL/U, peripheral T-cell lymphoma unspecified.

Sample	Diagnosis	Tissue	CRTC2 IHC
FFPE			
1	ATCL	Lymph node, right cervical, biopsy	Negative
2	ATCL	Lymph node, biopsy	Negative
3	ALCL	Retroperitoneal mass	Negative
4	ATCL	Lymph node, biopsy	Negative
5	ATCL	Lymph node excision	Negative
6	ATCL	Lymph node, inguinal, biopsy	Negative
7	ALCL	Mass, right iliac fossa, needle core biopsy	Negative
8	PTCL/U	Retroperitoneal lymph node	Negative
9	ALCL	Right anterior axillary lymph node, biopsy	Negative
10	ALCL	Left thigh, core biopsies	Negative
11	PTCL/U	Spleen, splenectomy	Negative
12*	ATCL	Lymph node, left inguinal, biopsy	Negative
13	PTCL/U	Lymph node, left inguinal, biopsy	Negative
14	ATCL	Lymph node, right cervical, excision	Negative
15	ATCL	Lymph node, left inguinal, excision	Negative
16	ATCL	Lymph node, left axillary, excision	Positive
17	ATCL	Lymph node, left cervical, biopsy	Negative
18	ALCL	Lymph node (4R), biopsy	Negative
19	ALCL	Lymph node, right inguinal region	Negative
20*	ALCL	Skin, right and left leg, punch	Negative
21	PTCL/U	Right parotid mass, excisional biopsy	Negative
22	PTCL/U	Lymph node, biopsy	Negative
23*	ALCL	Skin, right upper posterior thigh	Negative
24	ALCL	Right axillary lymph node, excision	Negative
Snap-frozen			
A	ALCL	Lymph node excision	N/A
B	ALCL	Retroperitoneal mass	N/A
C	ATCL	Lymph node, inguinal, biopsy	N/A
D	PTCL/U	Retroperitoneal lymph node	N/A
E	PTCL/U	Lymph node excision	N/A
F	ATCL	Lymph node (left cervical), biopsy	N/A
G	PTCL/U	Lymph node, biopsy	N/A

* Indicates primary cutaneous lymphoma.

SUPPLEMENTAL EXPERIMENTAL PROCEDURES

Cell Lines and Culture

HEK293T and NIH 3T3 cells (ATCC) were cultured in DMEM or DMEM with 10% FBS, respectively. For drug treatments, HEK293T or HeLa cells were treated with 10 μM forskolin (Sigma) for 4 hours or UV (30 J/cm^2). Plasmids expressing wild-type CRTC2 or CRTC2-S171A (Screaton et al., 2004), or wild-type CREB1 or CREB1-S133A (Du et al., 2000) were provided by Marc Montminy (Salk Institute).

shRNA-Mediated Knockdown

Cells were stably transduced with short hairpin RNA (shRNAs) viruses from Open Biosystems/GE Dharmacon listed below. Infected cells were then selected with puromycin.

List of Catalog Numbers for shRNAs Obtained from Open Biosystems/GE Dharmacon

Gene	First shRNA	Second shRNA
CRTC2 (human)	V3LHS_379706	V3LHS_379707
CREB1 (human)	TRCN0000007310	TRCN0000011085
CBP (human)	TRCN0000011027	TRCN0000006488
Crtc2 (mouse)	TRCN0000173279	TRCN0000176130
Msh6 (mouse)	TRCN0000071163	TRCN0000071165
Exo1 (mouse)	TRCN0000071123	TRCN0000071124

Real-Time qRT-PCR

Total RNA was isolated, and reverse transcription was performed as described previously (Gazin et al., 2007), followed by real-time qPCR with Platinum SYBR green qPCR SuperMix-UDG with Rox (Invitrogen) using the primers listed below.

List of Primers Used for qRT-PCR

Gene	Forward (5' → 3')	Reverse (5' → 3')
CRTC2 (human)	CCACCAGAACTTGACCCACT	GGCTGCTGCAATCTCCTTAG
Crtc2 (mouse)	CCACCAGAACTTGACCCACT	GGCTGCTGCAATCTCCTTAG
EXO1 (human)	AGCTTGGGGATGTATTCACG	TGCCTTTGCTAATCCAATCC
Exo1 (mouse)	CAGGCTGTCATCACAGAGGA	CTGGTCCACTTCCAGTCCAT
MSH6 (human)	GGAGGAAGGAAGCAGTGATG	CATTCTCTTCCGCTTTCGAG
Msh6 (mouse)	CTGCCATCAGTGACCGTCTA	TCAAGGTCTGGCAGCTTCTT
PMS1 (human)	GGCTGTTGATGCACCTGTAA	GCTTCTCCACGAAAACCGTA
Pms1 (mouse)	TGGAATCTGTTGAGCAGCAC	GGGGTTGAAAGACTTGTGGA
POLD2 (human)	GAGACCCTTCCTGGAGAACC	CCACACAGCACTTCTCCTCA
Pold2 (mouse)	CAGTGTGGAGGCAGTCAAAA	AGTTGGTGGGATCAAACTCG

Spontaneous Mutation Frequency

The *HPRT* mutation assay was conducted as described previously (Kat et al., 1993). Briefly, 5×10^6 cells were seeded in triplicate in 100 mm dishes for 12 hr and fed with complete medium containing 5 μM freshly prepared 6-thioguanine (6-TG; Sigma). The plating efficiency was determined by culturing 5×10^2 cells similarly in the absence of 6-TG. After 10 days of culturing, cell colonies were visualized by staining with 0.03% crystal violet. The mutation frequency was

determined by dividing the number of 6-TG-resistant colonies by the total number of cells plated after being corrected for colony-forming ability.

ChIP Assays

ChIP assays were performed as previously described (Raha et al., 2005) using an anti-CRTC2 (Bethyl Laboratories), anti-CREB1 (Cell Signaling Technology), anti-CBP (Bethyl Laboratories) or anti-histone H3 (acetyl K9+K14+K18+K23+K27) (Abcam, ab47915) antibody. ChIP products were analyzed by qPCR using primers listed below. Samples were quantified as percentage of input, and then normalized to an irrelevant region in the genome (~3.2 kb upstream from the transcription start site of *GCLC*). Fold enrichment was calculated by setting the IgG control IP sample to 1.

List of Primers Used for ChIP

Gene	**Forward (5' → 3')**	**Reverse (5' → 3')**
EXO1	CGTTGACGTCACATCCTCTG	ACGCAGAACACGGGTAACTT
MSH6	CCCGGCCTCTCATAGTCTCT	TAAGGGCCACAGTCCGTTAT
PMS1	CTGGGCCAGAGAAAACTCAG	ACGCAAATCCTCGTTGTCTT
POLD2	CAGGAAACCGAGGGTGTG	CCATCGCCTAATCTCACCAA

PAT-ChIP

Formalin-fixed paraffin-embedded tonsil (n=7) and lymphoma (n=24) sections were deparaffinized, rehydrated, and processed as previously described (Fang et al., 2014) using an anti-histone H3 (acetyl K9+K14+K18+K23+K27) (Abcam, ab47915) antibody. PAT-ChIP products were analyzed by qPCR using CRTC2 forward (TCTCAGGGAGTAGCCGAGAG) and reverse (CAGTCACGCAGCACTAGGAG) primers.

Colony Formation Assays

NIH 3T3 cells (1×10^4) stably expressing an shRNA were plated in 60-mm dishes and selected with puromycin for 14 days. Colonies were stained with crystal violet and counted.

SUPPLEMENTAL REFERENCES

Arredouani, M.S., Lu, B., Bhasin, M., Eljanne, M., Yue, W., Mosquera, J.M., Bubley, G.J., Li, V., Rubin, M.A., Libermann, T.A*., et al.* (2009). Identification of the transcription factor single-minded homologue 2 as a potential biomarker and immunotherapy target in prostate cancer. Clin. Cancer Res. *15*, 5794-5802.

Du, K., Asahara, H., Jhala, U.S., Wagner, B.L., and Montminy, M. (2000). Characterization of a CREB gain-of-function mutant with constitutive transcriptional activity in vivo. Mol. Cell. Biol. *20*, 4320-4327.

Fang, M., Ou, J., Hutchinson, L., and Green, M.R. (2014). The BRAF oncoprotein functions through the transcriptional repressor MAFG to mediate the CpG Island Methylator phenotype. Mol. Cell *55*, 904-915.

Gazin, C., Wajapeyee, N., Gobeil, S., Virbasius, C.M., and Green, M.R. (2007). An elaborate pathway required for Ras-mediated epigenetic silencing. Nature *449*, 1073-1077.

Graudens, E., Boulanger, V., Mollard, C., Mariage-Samson, R., Barlet, X., Gremy, G., Couillault, C., Lajemi, M., Piatier-Tonneau, D., Zaborski, P*., et al.* (2006). Deciphering cellular states of innate tumor drug responses. Genome Biol. *7*, R19.

Karnoub, A.E., Dash, A.B., Vo, A.P., Sullivan, A., Brooks, M.W., Bell, G.W., Richardson, A.L., Polyak, K., Tubo, R., and Weinberg, R.A. (2007). Mesenchymal stem cells within tumour stroma promote breast cancer metastasis. Nature *449*, 557-563.

Kat, A., Thilly, W.G., Fang, W.H., Longley, M.J., Li, G.M., and Modrich, P. (1993). An alkylation-tolerant, mutator human cell line is deficient in strand-specific mismatch repair. Proc. Natl. Acad. Sci. USA *90*, 6424-6428.

Mayr, B., and Montminy, M. (2001). Transcriptional regulation by the phosphorylation-dependent factor CREB. Nat. Rev. Mol. Cell Biol. *2*, 599-609.

Piccaluga, P.P., Agostinelli, C., Califano, A., Rossi, M., Basso, K., Zupo, S., Went, P., Klein, U., Zinzani, P.L., Baccarani, M*., et al.* (2007). Gene expression analysis of peripheral T cell lymphoma, unspecified, reveals distinct profiles and new potential therapeutic targets. J. Clin. Invest. *117*, 823-834.

Raha, T., Cheng, S.W., and Green, M.R. (2005). HIV-1 Tat stimulates transcription complex assembly through recruitment of TBP in the absence of TAFs. PLoS Biol. *3*, e44.

Screaton, R.A., Conkright, M.D., Katoh, Y., Best, J.L., Canettieri, G., Jeffries, S., Guzman, E., Niessen, S., Yates, J.R., 3rd, Takemori, H*., et al.* (2004). The CREB coactivator TORC2 functions as a calcium- and cAMP-sensitive coincidence detector. Cell *119*, 61-74.

Sun, L., Hui, A.M., Su, Q., Vortmeyer, A., Kotliarov, Y., Pastorino, S., Passaniti, A., Menon, J., Walling, J., Bailey, R*., et al.* (2006). Neuronal and glioma-derived stem cell factor induces angiogenesis within the brain. Cancer Cell *9*, 287-300.

Wang, Q., Wen, Y.G., Li, D.P., Xia, J., Zhou, C.Z., Yan, D.W., Tang, H.M., and Peng, Z.H. (2012). Upregulated INHBA expression is associated with poor survival in gastric cancer. Med. Oncol. *29*, 77-83.